

# Aggregation behavior of a lattice model for amphiphiles

Allan D. Mackie<sup>†</sup>, Athanassios Z. Panagiotopoulos\*

*School of Chemical Engineering, Cornell University, Ithaca, NY 14853-5201, USA.*

and Igal Szleifer

*Department of Chemistry, Purdue University, Lafayette, IN, 47907, USA.*

(June 16, 1997)

## I. ABSTRACT

We have studied aggregation of a lattice model for amphiphiles due to Larson using Monte Carlo simulations and single-chain mean-field theory. Near-spherical micellar aggregates form spontaneously in the simulations. In contrast to standard equilibrium theories, our simulations show a decrease in free monomer concentration above the critical micelle concentration. This phenomenon is probably due to non-ideal mixing effects in solution. The structure of micelles of a given aggregation number predicted by the theory is in excellent agreement with simulation results. The single-chain mean-field theory also accurately predicts the critical micelle concentration. The mean-field prediction for the distribution of micelle size is sharper and is peaked at lower values than simulation results. We suggest ways to modify the theory to improve agreement with simulation.

## II. INTRODUCTION

Micellar aggregates are often observed in dilute solutions of amphiphiles in solvents in which it is thermodynamically favorable for the amphiphiles to form long-lived aggregates. Micellar geometries that are observed include spheres, cylinders, and bilayer discs<sup>1</sup>. In order to simulate micellar solutions, large system sizes are required so that there are sufficient amphiphiles to allow the formation of several micelles in a sufficiently dilute amphiphile solution.

Detailed atomistic models have been proposed for the study of single micelles<sup>2-4</sup>, however even today's computers lack the speed required to study large systems of micelles for these models. Simplified models have been provided for which self-assembly can be simulated in a reasonable time. For example, in the work by Smit *et al.*<sup>5-8</sup> the amphiphiles are considered to be chains of Lennard-Jones spheres in continuous space. More commonly, a lattice approximation is used and the amphiphiles are represented by chains of connected sites<sup>9-13</sup>. These models are a reasonable representation of non-ionic amphiphiles rather than the more common ionic surfactants. Several simulation groups have observed that under the right conditions these models form peaks in their cluster distributions<sup>7,12,14-17</sup>. The formation of peaks is

often taken to be a good criterion for the identification of micellar-type aggregates<sup>1</sup>.

Having already investigated in a previous paper<sup>18</sup> the phase behavior of one of these models proposed by Larson<sup>9</sup>, we are in a good position to investigate micellization for the same model. Since the investigations are carried out in the canonical (NVT) ensemble, care has to be taken to avoid simulating densities that fall within phase-separated regions. If the density lies within such a region, a peak in the cluster distribution may form. However, rather than being indicative of micelle formation, it would be the beginning of the formation of a second phase. As the simulation system size is increased, this peak will move towards higher aggregation numbers and become infinite in the thermodynamic limit. In contrast, a micellar peak should stay at approximately the same aggregation number.

The present paper has some similarities with a recent independent study by Wijmans and Linse<sup>14</sup>. They use a cubic lattice model with a lower coordination number than ours and a different mean-field theory. Comparison of the two studies provides insights into the effects of the model used on the observed micellization behavior and on the relative performance of the theories.

In this paper, we first describe the amphiphile model and the simulation techniques, in particular a cluster move used to displace whole aggregates. A statistical thermodynamic theory is presented for the properties of aggregates of a given geometry. Structural properties of the amphiphiles, such as the density profiles and the free energy of formation of a single aggregate can be obtained from the theory. The theory assumes that whole chains interact with the other chains and solvent in a mean-field way. The geometry of the aggregate has to be specified, but the size of the aggregate is determined by the theory, i.e. the interface is not assumed to be sharp. No other approximations are made and no adjustable parameters are introduced. The standard chemical potentials of formation from the single-chain mean-field theory combined with the multiple equilibrium model in the ideal solution limit are used to determine the critical micellar concentration and the size distribution of micelles. In the results section, we present our findings from the simulations, and compare them to calculations based on the mean-field theory. We conclude with a discussion of possible ways to improve agreement between theory and simulation.

### III. MODEL

In the model studied here, originally proposed by Larson<sup>9</sup>, space is discretized into a cubic lattice of sites in three dimensions. Solvent molecules occupy single sites whereas amphiphile molecules occupy chains of connected sites. Interactions of equal magnitude occur on vectors (0,0,1), (0,1,1), (1,1,1) on the lattice and the vectors resulting from symmetry operations along the  $x$ ,  $y$ , and  $z$  axes (26 in total). The connected sites along the amphiphile backbone are restricted to be on the same vectors. This results in chains with significantly higher flexibility than the “standard” cubic lattice model, so that even short chains can form stable aggregates. The abbreviation  $H_xT_y$  is used to denote an amphiphile which has  $x$  head sites and  $y$  tail sites. A water-like solvent particle is denoted by H and an oil-like particle by T. Unfavorable interactions exist between “oil” and “water” particles, leading to liquid-liquid demixing in the absence of amphiphile.

In the present paper, all systems studied are binary mixtures of amphiphile and H-monomers. The lattice is fully occupied. If an H-type site belonging to a water monomer or the head of an amphiphile interacts with another H-type site the resulting energy is  $\epsilon_{ww}$ . The T-T and H-T interaction energies are denoted by  $\epsilon_{oo}$  and  $\epsilon_{wo}$ . There is only one relevant energy parameter,  $\epsilon = \epsilon_{wo} - \frac{1}{2}\epsilon_{ww} - \frac{1}{2}\epsilon_{oo}$ . The dimensionless temperature is defined using this energy parameter,  $T^* = kT/\epsilon$ , where  $k$  is Boltzmann’s constant.

### IV. SIMULATION METHODOLOGY

Micellization is a single phase phenomenon observed at low concentrations of amphiphilic molecules. We therefore used large-scale canonical (NVT) simulations. The simulations ranged in size from lattices of  $40^3$  up to  $120^3$  in which periodic boundary conditions were implemented in all three dimensions. We considered only mixtures of amphiphile and H-sites. Introducing “oil” (T-sites) into the system presents no significant difficulties but does add another variable. The main challenge in these simulations is that the chains exist at low concentrations but also form aggregates. In order to sample phase space efficiently it was necessary to consider moves which displace both monomers and aggregates. We used reptation and chain regrowth to move the amphiphilic molecules<sup>18</sup>.

We implemented a cluster move in the spirit of the Swendsen and Wang algorithm<sup>20,21</sup> to move micellar aggregates efficiently. In the cluster move, whole clusters are shifted by one site in a random direction in a manner that maintains detailed balance. An amphiphile is considered to be part of a cluster if any of its tails segments is in a neighboring site of a tail segment from another amphiphile. In the Appendix a derivation is given of the acceptance probabilities needed to maintain detailed

balance during a cluster move. This derivation and move follows the treatment of Wu *et al.*<sup>22</sup>. A typical mix of the Monte Carlo moves used was 80% reptations, 19.99% regrowth, and 0.01% cluster moves. Simulations were carried out for at least  $5 \times 10^8$  Monte Carlo steps which require approximately 30 hours on an IBM RS6000 workstation.

During the simulations, we keep track of several quantities. These include the cluster distribution, radii of gyration of the aggregates, and density profiles through the aggregates. The radii of gyration tensor is a useful measure of the size and shape of an aggregate and is defined by<sup>24</sup>,

$$R_{\gamma,\delta}^2 = \frac{1}{N_{cl}} \sum_{i=1}^{N_{cl}} (\gamma_i - \gamma_{cm})(\delta_i - \delta_{cm}) \quad (1)$$

where  $\gamma, \delta = x, y, z$  coordinates, the subscript  $cm$  denotes the center of mass of the aggregate, and  $N_{cl}$  is the number of sites in the aggregate. Rather than quoting the whole tensor, it is useful to consider the three principal radii of gyration, or rather the three eigenvalues of the tensor. These radii,  $R_1^2, R_2^2, R_3^2$  in descending order of magnitude, are averaged in the course of a simulation.

### V. MULTIPLE EQUILIBRIUM MODEL

The critical micellar concentration as well as the size and shape distribution of micelles can be, in principle, determined from the condition that at thermodynamic equilibrium the chemical potential of the amphiphiles must be the same whether they form micelles or are in the form of monomers in solution.

The chemical potential of amphiphiles in aggregates with  $N$  molecules,  $\mu_N$ , can be expressed

$$\mu_N = \mu_N^0 + \frac{k_B T}{N} \ln \left( \frac{\gamma_N X_N}{N} \right), \quad (2)$$

where  $\mu_N^0$  is the standard chemical potential,  $\gamma_N$  is the activity coefficient of an amphiphile in an aggregate containing  $N$  amphiphiles and  $X_N$  is the mole fraction of amphiphiles incorporated into these aggregates.

The condition of thermodynamic equilibrium requires<sup>1</sup>

$$\mu_1 = \mu_2 = \mu_3 = \dots = \mu_N = \mu = const. \quad (3)$$

which can be converted, using the explicit form (2), to

$$X_N = N(\gamma_1 X_1)^N \exp [N(\mu_1^0 - \mu_N^0)/k_B T] / \gamma_N. \quad (4)$$

In general there is no simple way in which the activity coefficients of the aggregates can be determined. These coefficients contain information on the inter-aggregate interactions. By assuming ideality, the activity coefficients are set equal to one so that Eq. (4) becomes,

$$X_N = N(X_1)^N \exp [N(\mu_1^0 - \mu_N^0)/k_B T]. \quad (5)$$

The size distribution is thus determined by the difference in standard chemical potentials between the monomer and the amphiphiles in the aggregate,  $\mu_1^0 - \mu_N^0$ . The preferred geometry is chosen on the basis of the difference of the  $\mu_N^0$  for the different geometries,  $\mu_N^0$  being a function of geometry. The total amphiphile mole fraction is  $X = \sum_i X_i$ . The mole fraction of any component  $i$ ,  $X_i$ , is related to the volume fractions,  $\phi_i$  through

$$X_i = \frac{\phi_i/n_i}{\sum_i \phi_i/n_i}, \quad (6)$$

where the sum is taken over all components in the system and  $n_i$  is the number of sites occupied by component  $i$ . In order to predict the aggregate distribution we need to know  $\mu_N^0$  for the different possible geometries, such as spherical, cylindrical, or bilayer for example. The preferred geometry will be the one which has the lowest chemical potential.

The standard chemical potential,  $\mu_N^0$ , can be understood as the free energy per molecule of an aggregate of size  $N$  that has no interactions with the other aggregates and monomers and is fixed in space, i.e. a micelle in an ideal solution that has its translational motion frozen. This quantity includes all the intermolecular interactions *within* the aggregate. Therefore, it should be clear that the ideality assumption,  $\gamma_i = 1$ , concerns only the *inter*-aggregate interactions which will be a good assumption if the solution is dilute enough in aggregates and monomers. There are still many non-ideal intra-aggregate terms which need to be considered to properly estimate the standard chemical potentials. In this work we approximate the standard chemical potential with the free energy of a chain in the mean-field of the other chains in the aggregate and neglect the other intra-aggregate terms such as the rotational motion of the aggregate<sup>23</sup>.

We now turn to the single-chain mean-field theory that enables us to calculate the standard chemical potentials as well as the molecular organization in the aggregate. In the results section we show how the predictions of the theory compare with the results from simulations.

## VI. SINGLE-CHAIN MEAN-FIELD THEORY

The single-chain mean-field (SCMF) theory is an approach originally developed to treat the packing of chain molecules in amphiphilic aggregates<sup>25,26</sup> and later generalized to study the molecular organization and thermodynamic properties of polymer molecules close or attached to surfaces<sup>29,30</sup>. The basic idea of the theory is to look at a central chain with all its intramolecular interactions exactly taken into account while the intermolecular interactions are considered within a mean-field approximation. Since a micellar aggregate is clearly inhomogeneous the intermolecular mean-field interactions are also inhomogeneous. The theory is derived by determining the

probability distribution function (pdf) of chain conformations by minimization of the aggregate's free energy subject to the lattice single occupancy constraint. It is important to note that we do not restrict the boundary of the aggregate, as was done in earlier versions of this theory for amphiphilic aggregates<sup>25,26,28</sup>, instead the size of the aggregate for a given geometry is a prediction given by the minimal free energy of the aggregate.

One of the main advantages of the SCMF theory is that the chain molecules are the basic units, i.e. the amphiphiles are treated as a whole. As a result: (i) the reference state of the system which is composed by isolated chains in the solvent is properly calculated; (ii) the chain connectivity is exactly taken into account enabling the proper counting of interacting neighbors (both intra and intermolecular), and the exact intramolecular self-avoidance; and (iii) the chain structure is independent of the geometry of the aggregate. Therefore, this theory is not limited to lattice chains but actually most of its applications have been for off-lattice chains for a large variety of chain models including realistic lipids and surfactant molecules<sup>27,31</sup>

Another theoretical approach frequently used for the packing of chain molecules is the self-consistent field (SCF) theory of Scheutjens and Fleer<sup>32,33</sup> as applied by Leermakers<sup>34</sup> to amphiphilic aggregates. In their approach the chains are generated by the Green's function of a random walk in the presence of the interacting mean-field. Namely, the intra and inter-molecular interactions are not separated since the basic unit in their approach is a monomer and not the whole amphiphile. While this results in a simpler computational methodology, their approach leads to Flory's solution in the bulk, i.e. the chains follow Gaussian statistics resulting in an inappropriate estimate of the free energy of the system for bulk and small deviations from bulk<sup>30</sup>. For relatively short amphiphiles such as the ones used in the present work, the Gaussian statistics for the chains are probably not the appropriate ones<sup>30</sup> and they are believed to lead to inaccurate density profiles of the micelles<sup>14</sup>. In addition, in the Scheutjens-Fleer-Leermakers approach, the amphiphiles and solvent are restricted to a lattice with a geometry constrained to that of the aggregate.

We now present a short derivation of the SCMF theory as applied to the packing of amphiphiles modeled by the same chain model as the Monte Carlo simulations. We need to write the free energy of an aggregate fixed in space, in terms of the pdf of chain conformations,  $P(\alpha)$ , where  $\alpha$  is the chain conformation. In order to do so we discuss each of the contributions to the thermodynamic potential.

The intermolecular repulsions are taken into account through the single occupancy condition. Namely, each lattice site can be occupied by a solvent, a tail segment or a head segment. We will consider here only spherical aggregates for which only the radial direction is inhomogeneous, due to the spherical symmetry of the aggregate. Thus, we divide the aggregate in concentric layers

as shown in Fig. 1. The packing constraints, or repulsive (single occupancy) interactions are given by

$$\phi_s(r) + \langle \phi(r) \rangle = 1 \quad \text{for all } r; \quad (7)$$

where  $\langle \rangle$  denote an average over the pdf of chain conformations;  $\phi_s(r)$  is the volume fraction of solvent and  $\langle \phi(r) \rangle = \frac{N}{V(r)} (\langle n_H(r) \rangle + \langle n_T(r) \rangle)$  is the chains volume fraction, with  $V(r)$  being the number of lattice sites in layer  $r$  and  $\langle n_{H(T)}(r) \rangle$  denotes the average number of head (tail) segments per chain in layer  $r$ .

We can now write the attractive contribution to the interaction energy. It is convenient to consider the case where all the interactions are between the tails of the amphiphiles so that  $\epsilon_{ww} = 0$  and  $\epsilon_{ow} = 0$ . Since there is only one relevant energy scale,  $\epsilon$ , this merely rescales the energy. The intramolecular "attractive" interaction per chain in the aggregate is

$$\langle E_{intra} \rangle = \epsilon_{oo} \langle n_{TT}^{int} \rangle = \epsilon_{oo} \sum_{\alpha} P(\alpha) n_{TT}^{int}(\alpha) \quad . \quad (8)$$

where  $\langle n_{TT}^{int} \rangle$  is the average number of intramolecular tail-tail contacts per chain and where the summation is taken over the set of all possible chain configurations  $\alpha$ .

The intermolecular interaction term is written in a mean-field approximation. Namely, we take the probability of having a neighboring site to a tail segment of the central chain occupied by a tail segment of another chain, be given by the average *local* density of tail segments. Note, that this is non-local since the average density of segments is inhomogeneous in the radial direction. Thus, the intermolecular attractive contribution can be written as

$$\langle E_{inter} \rangle = \frac{\epsilon_{oo}}{2} \sum_r \langle n_{n,T}(r) \rangle \langle \phi_T(r) \rangle \quad (9)$$

where  $\langle n_{n,T}(r) \rangle$  is the average number of non-occupied nearest-neighbor contacts in shell  $r$  per chain,  $\langle \phi_T(r) \rangle = \frac{N}{V(r)} \langle n_T(r) \rangle$  is the average tail (probability) volume fraction in shell  $r$ . The division by a factor of two fixes the double counting in the chain-chain contacts.

The last term needed to determine the aggregate's free energy is the entropy. This term contains two contributions, the conformational entropy of the amphiphiles and the translational entropy of the solvent molecules. They are

$$\frac{S}{k_B} = -N \sum_{\alpha} P(\alpha) \ln P(\alpha) - \sum_r n_s(r) \ln \phi_s(r) \quad (10)$$

where  $\phi_s(r)$  is the volume fraction of solvent, and  $n_s(r)$  is the number of solvent sites, both at layer  $r$ .

The configurational free energy of the aggregate is,

$$\begin{aligned} \frac{F}{k_B T} &= \beta N [\langle E_{intra} \rangle + \langle E_{inter} \rangle] - \\ &- \frac{S}{k_B} - \beta \sum_r n_s(r) \mu_s, \end{aligned} \quad (11)$$

where the last term is necessary since effectively the aggregate is considered to be in contact with a bath of pure solvent with chemical potential  $\mu_s$ .

The pdf,  $P(\alpha)$ , and solvent density profile,  $\phi_s(r)$ , are found by minimization of the free energy, (11), subject to the packing constraints, (7) where the definitions of the intermolecular and intramolecular energies (Eqs. (8) and (9)) are substituted into Eq.(11). This is done by introducing the set of Lagrange multipliers  $\{\pi(r)\}$  to give

$$\begin{aligned} P(\alpha) &= \frac{1}{q} \exp\{-\sum_r \pi(r)[n_H(r, \alpha) + n_T(r, \alpha)] - \\ &- \chi_{oo} n_{TT}^{int}(\alpha) - \frac{\chi_{oo}}{2} \sum_r \frac{N}{V(r)} [n_{n,T}(r, \alpha) \langle n_T(r) \rangle + \\ &+ \langle n_{n,T}(r) \rangle n_T(r, \alpha)]\} \end{aligned} \quad (12)$$

where

$$\begin{aligned} q &= \sum_{\alpha} \exp\{-\sum_r \pi(r)[n_H(r, \alpha) + n_T(r, \alpha)] - \chi_{oo} n_{TT}^{int}(\alpha) \\ &- \frac{\chi_{oo}}{2} \sum_r \frac{N}{V(r)} [n_{n,T}(r, \alpha) \langle n_T(r) \rangle + \\ &+ \langle n_{n,T}(r) \rangle n_T(r, \alpha)]\} \end{aligned} \quad (13)$$

is the normalization constant that ensures  $\sum_{\alpha} P(\alpha) = 1$  where the sum is taken over the set of all possible chain configurations, and where we have defined the dimensionless interaction parameter  $\chi_{oo} = \beta \epsilon_{oo}$ .

The solvent density profile is given by

$$\phi_s(r) = \exp[-\pi(r) + \beta \mu_s] \quad (14)$$

where the thermodynamic equilibrium condition that the chemical potential of the solvent,  $\mu_s$ , must be constant at all  $r$  has been introduced.

The expression for the solvent density profile gives us the physical interpretation of the Lagrange multipliers. They are the osmotic pressures necessary to keep the chemical potential of the solvent constant at all  $r$ . For a detailed discussion of the meaning of these quantities see ref.<sup>30</sup>.

The expressions for the solvent volume fraction profile and the probabilities can be substituted back into the free energy expression, Eq. (11), to obtain

$$\begin{aligned} \frac{F}{k_B T} &= -N \frac{\chi_{oo}}{2} \sum_r \frac{N}{V(r)} \langle n_{n,T}(r) \rangle \langle n_T(r) \rangle - \\ &- N \ln q - \sum_r \pi(r) V(r) \end{aligned} \quad (15)$$

The standard chemical potential needed in the multiple equilibrium model, Eq. (4), to obtain the cmc and the micellar size distribution is given by

$$\frac{\mu_N^0}{k_B T} = \frac{\partial(F/k_B T)}{\partial N} = -\ln q - n \quad (16)$$

where  $n$  is the number of sites occupied by an amphiphile and is constant.

Any average property of interest,  $A$ , of the chains can be calculated from the  $P(\alpha)$ 's in the form

$$\langle A \rangle = \sum_{\alpha} P(\alpha) A(\alpha) . \quad (17)$$

The only remaining task is to find the lateral pressures  $\pi(r)$ . In order to do this we substitute the explicit form of the pdf, Eq. (12), and that of the solvent density profile, Eq. (14), into the constraint equations, Eq. (7), and obtain

$$\begin{aligned} & \sum_{\alpha} \frac{1}{q} \exp\left\{-\sum_r \pi(r)[n_H(r, \alpha) + n_T(r, \alpha)] - \chi_{oo} n_{TT}^{int}(\alpha)\right. \\ & - \frac{\chi_{oo}}{2} \sum_r \frac{N}{V(r)} [n_{n,T}(r, \alpha) \langle n_T(r) \rangle + \\ & + \langle n_{n,T}(r) \rangle n_T(r, \alpha)] \left. \right\} \frac{N}{V(r)} (n_H(r, \alpha) + n_T(r, \alpha)) + \\ & + \exp[-\pi(r) + \beta \mu_s] = 1 \quad \forall r \end{aligned} \quad (18)$$

which is a set of non-linear self-consistent equations that can be solved by standard numerical methods. The input necessary to solve these equations are: (1) the set of single chain conformation of the amphiphile molecules. (2) the number of amphiphiles in the aggregate and (3) the solvent chemical potential. It turns out that the solvent chemical potential is not necessary to solve the equations<sup>30</sup>. Actually, since  $\mu_s$  can be considered the chemical potential of the pure solvent its value is equal to zero in our lattice model.

The amphiphile configurations are obtained using the Rosenbluth and Rosenbluth chain growth algorithm<sup>36</sup>. It is important to note at this point that the set of configurations  $\alpha$  include the different possible bond sequences and also the position of the chain with respect to the center of the aggregate. Once we have a set of configurations they can be placed onto the lattice and the chain distributions counted as a function of radius from the aggregate center. In Fig. 1, a two dimensional schematic diagram is given of the way that chains are placed on a lattice to count the distribution of segments. The shell volumes are defined by counting the number of sites included in each layer. A site is considered to be included in a shell if the center of the site falls within the shell as defined in continuous space.

We generated  $5 \times 10^4$  amphiphile configurations using the Rosenbluth and Rosenbluth chain growth algorithm<sup>36</sup> and placed them on a lattice divided into spherical shells, as shown in two dimensions in Fig. 1, so that the distribution of tails, heads and nearest neighbor contacts can be obtained for each configuration. The same results were obtained when  $10^5$  configurations were used. A representative set of positions for the first tail segment on the lattice needs to be chosen to fairly represent the complete set. The complete set would be where

the first tail segment is placed on every lattice site that is not related by symmetry. The first tail segment of the configurations were placed at four different radii on the diagonal and straight as well as their symmetrically inverted configurations for a total of sixteen different positions for each configuration. Symmetrically inverted implies that chains are inverted about the center of the chain so that configurations which originally had their tails pointing to the center now have the tails pointing outwards and their heads towards the center. The chemical potential of the monomer is calculated by summing over the set of configurations only, without the summation over positions and in the presence of pure solvent.

## VII. RESULTS AND DISCUSSION

### A. Simulation

The simulations were performed at the same temperature,  $kT/\epsilon = 6.5$ , as was used for the phase diagrams in our previous work<sup>18</sup>. We investigated all of the amphiphiles studied in the paper on phase behavior, namely  $H_1T_1$ ,  $H_2T_2$ ,  $H_4T_4$ , and  $H_1T_3$ ,  $H_2T_4$ ,  $H_2T_6$ , but only in the case of the  $H_4T_4$  amphiphile did we find peaks in the cluster distributions indicative of micellar formation. Since only one temperature was studied there is the possibility that aggregates may form at other temperatures. In the case of the symmetric amphiphiles,  $H_1T_1$  and  $H_2T_2$ , it appears that they are too small to form large aggregates, in line with Larson's conclusions<sup>15</sup>. For the asymmetric amphiphiles, the search is restricted to low amphiphile concentrations which fall below the two-phase region of the phase diagrams previously determined<sup>18</sup>. The low solubility of  $H_2T_6$  as predicted from the quasi-chemical theory requires that larger lattices than can presently be simulated be used. We were thus unable to investigate the micellization of  $H_2T_6$ . Both the  $H_1T_3$  and  $H_2T_4$  amphiphiles fall within the bounds of reasonable solubilities as far as simulation is concerned. Although preliminary investigations did not reveal micellization, further work is required to confirm this.

In light of the lack of observed aggregation for all but the  $H_4T_4$  amphiphile, our studies focused on this one amphiphile. The ternary phase diagram for  $H_4T_4 - H - T$ <sup>18</sup> from the Monte Carlo results suggests that the amphiphile and water are completely soluble over the whole composition range when no oil is present. In other words there is no two-phase region. Even the quasi-chemical prediction, which tends to overestimate the amount of phase separation for these systems, shows a two-phase region that starts at approximately 8 vol.% amphiphile. At low amphiphile concentrations we can safely assume that we are not in a two-phase region. At higher amphiphile concentrations there is still the possibility for phase transitions occurring that are too subtle for the methods used in our previous paper<sup>18</sup> to detect, such

as transitions from packed spheres to infinite cylinders. These transitions are difficult to find in simulations for several reasons. First of all, the interfacial tension between these phases is very low which gives a small driving force for phase separation. Secondly, the length scales of self-assembled structures can be very large, even infinite in the case of infinite cylinders. Large system sizes are thus required in order to approximate the thermodynamic limit by an artificially periodic simulated system. In addition, the stability of the self-assembled structures makes it hard to sample phase space because it is difficult to perform moves that disrupt the structures which have a reasonable probability of acceptance.

Initial configurations were generated by putting amphiphile chains in place of water sites at random positions on a lattice. Initial chain conformations were obtained using the Rosenbluth and Rosenbluth chain growth algorithm<sup>36</sup> to avoid configurations with overlaps. It is important to maintain a simulation cell size that is large enough to allow the system to form aggregates typical of the solution in the thermodynamic limit of infinite system size. With this in mind, as the overall amphiphile concentration was decreased, the number of sites in the lattice was increased. We try to have at least five to ten micelles present in the systems that showed aggregation.

We obtained the cluster size distributions after the initial random configuration was equilibrated using the moves discussed in the section on methodology. Equilibration was checked for by observing that the same results could be obtained by starting from different initial configurations and by running the simulations for more Monte Carlo steps. A typical equilibrated configuration for a 1 vol. % amphiphile system on a  $120^3$  lattice is shown in Fig. 2 and a typical configuration for a system with 8 vol.% on a  $40^3$  lattice is given in Fig. 3. The micelles observed in both cases appear to be roughly spherical with the core of the micelle largely occupied by tail segments.

We have investigated the aggregate size distributions as a function of overall amphiphile volume fraction. In general, the volume fraction of an aggregate of size  $N$  decreases rapidly above the monomer and reaches a value close to zero above trimers. At higher aggregation numbers, micellar aggregates appear above an aggregation number of approximately  $N = 50$ . At overall volume fractions of amphiphile greater than 2%, (Fig. 4), we observe that the preferred aggregation number is approximately  $N = 80$ . As amphiphile overall loading increases above 2 vol %, more micelles of approximately the same size distribution form, confirming that the solution is truly micellar rather than phase-separated. However, we unexpectedly find that the peak in the size distribution shifts to higher aggregation numbers at overall surfactant concentrations lower than 2 %. This is in contrast to the predictions of multiple equilibrium models for ideal solutions which give a decrease in aggregate size when overall amphiphile concentration is reduced. Further work is under way to check this surprising result using Grand

Canonical Monte Carlo simulations. If we continue to decrease the total amphiphile concentration, we find that the peak in the cluster distribution eventually disappears. This happens for about 0.5 vol.% amphiphile.

The critical micelle concentration, or cmc, is defined as the point at which micelles appear in the system. Well below the cmc, no significant concentration of micelles can be found, even though there is, in principle, a finite probability of observing a cluster of any given size. Most of the amphiphile is present in the form of monomers. Above the cmc, as amphiphiles are added, the concentration of monomers stays roughly constant and the concentration of micelles increases. Since there is no true phase transition between the two states, the location of the cmc depends on the definition used to obtain it. For example, the cmc can be defined as the point at which half of the amphiphile is present in the form of chain clusters of two or more<sup>12</sup>, or when a maximum in the cluster distribution first forms<sup>39,40</sup>, when the electrical conductivity of the solution shows a sharp break<sup>41</sup>, or by using microcalorimetry to locate where the enthalpy of dilution shows a change of slope<sup>42</sup>, to name a few.

To locate the cmc for the  $H_4T_4 - H$  system, we plot the volume fraction of free chains, or monomers  $\phi_1$ , as well as the volume fraction of clusters larger than monomers,  $\phi_{N>1} = \sum_{i=2}^N \phi_i$ , against the total amphiphile concentration,  $\phi = \sum_{i=1}^N \phi_i$ , as in Fig. 5. The sum of the two quantities is equal to the total amphiphile concentration,  $\phi = \phi_1 + \phi_{N>1}$ . As can be seen, the monomer concentration comes to a maximum and then falls off as total amphiphile concentration is increased. The ideal multiple equilibrium model, Eq. (5), predicts that the monomer concentration should flatten out at the cmc and then slowly increase. The Monte Carlo results cannot be wholly explained by the multiple equilibrium model if we assume ideality of the solution. One possible reason for the decline is the decrease in free volume available to the monomers due to the presence of the aggregates. The free volume is defined as the volume left when the volume occupied by the aggregates is subtracted from the total volume. At the highest concentration of 16% amphiphile, the volume fraction of monomers in the free volume is 25% greater than the total volume fraction of monomers. This is not sufficient to significantly change the downward slope of the monomer concentration curve. The same qualitative behavior, namely a reduction of monomer volume fraction, has also been observed in simulations of other models<sup>12,45,46,17</sup>.

As was done by Stauffer *et. al.*<sup>12</sup> we define the cmc as being the total amphiphile concentration for which half of the surfactant is in the form of clusters of two or more amphiphiles. This is the concentration where the two curves plotted in Fig. 5 cross, namely 0.9 vol.% amphiphile.

In order to make a direct comparison with the mean-field theory, we need to make an assumption about the preferred geometry of the aggregates. During the simula-

tions we sampled the radii of gyration in order to obtain a quantitative measure of the aggregate shape. In Fig. 6 a plot of the principal radii of gyration as a function of aggregate size is given for a system at 1 vol.% amphiphile. Similar results were obtained for the system with 8 vol.% amphiphile. For the smaller aggregates the radii of gyration are approximately constant, but as the aggregate number increases the aggregates expand by increasing only one principle axis. That is, although the smaller aggregates are spherical, they increase in size by becoming cylindrical rather than forming larger spheres.

### B. Single-chain Mean-field theory

In this section the single chain mean-field theory is combined with the multiple equilibrium model to predict the cluster distributions and aggregate density profiles. The aggregate geometry needs to be specified to apply the single chain theory. The simplest choice is spherical aggregates since the radius is the only parameter affecting the size of a sphere. More complicated geometries, such as discs bounded by halved curved cylinders or cylinders capped with hemispheres, require more than one parameter to specify them completely and in the case of the cylinders require that the spherical case be solved first. From the plot of the radii of gyration, Fig. 6, it appears that the aggregates range from spherical to cylindrical. In this work we investigate only the case of spheres in the mean-field with the knowledge that this will probably be invalid for the larger aggregates. However, it is clear from the shape of the simulated aggregates that the geometry is rather complicated. Our aim is to see if the theory is able to predict the formation and structure of the micelles in the case of a well defined geometry, in this case spheres. We discuss below the possibilities of studying other geometries by mean-field theory and what would be expected in those cases.

The results for the density profiles for aggregates containing 80 monomers are shown in Fig. 7. The Monte Carlo data were taken by ensemble averaging the profiles for aggregates in a system containing 1 vol.% amphiphile. The density profile was not found to be a function of total amphiphile concentration. Symbols are plotted on the Monte Carlo results to identify the head, tail, and solvent density profiles. We find excellent agreement between the Monte Carlo result and the mean-field theory. Both Monte Carlo and mean-field theory show that the aggregates prefer to have a core packed almost exclusively with tail segments with a sharp interface between the core of tails and the rest of the system. The main difference between the two is that the Monte Carlo result shows a core that is slightly more diffuse at the interface than is found for the mean-field theory.

For larger aggregates we find that the Monte Carlo result becomes more diffuse compared to the mean-field theory, nevertheless agreement is still reasonable<sup>19</sup>. How-

ever, for aggregates large enough to be significantly non-spherical in shape, the mean-field theory continues to predict a core of tail segments with a relatively sharp interface whereas the Monte Carlo result shows a broad distribution with tail segments found at large distances away from the center of mass of the aggregate. This is a direct consequence of the non-spherical geometry of the aggregates and therefore the comparison with the theory applied for spherical aggregates is meaningless.

The chemical potential of the amphiphiles within the aggregate determine the size and shape distribution. In principle it should be possible to find the standard chemical potential of aggregates in a simulation by performing test particle insertions and attributing energies to clusters contacted during the insertion. Unfortunately, we find that we obtain poor statistics from such a scheme. Another approach is possible if we assume ideality of the micellar solution and use the multiple equilibrium model. Eq. (3) gives a relationship between the standard chemical potential of aggregates and the cluster distribution and can be rewritten to give,

$$\mu_N^0 = \mu - \frac{k_B T}{N} \ln \left( \frac{X_N}{N} \right) \quad (19)$$

where  $\mu$  is the chemical potential of amphiphile in solution (equal for all aggregate sizes) and the activity coefficients have been set to one. Since the overall chemical potential is constant for a given amphiphile concentration, we can use the cluster profiles already found from the simulations for the  $\phi_N$  to obtain the standard chemical potentials as a function of aggregate size  $N$ . In Fig. 8 we plot the predictions from the single chain mean-field theory and the result from inverting the Monte Carlo size distribution for 1 and 8 vol.% amphiphile. Absolute chemical potential is arbitrary so we chose to match the monomer chemical potential for all three distributions. The mean-field theoretical result gives a minimum at around 55 chains. In contrast, the Monte Carlo results are much flatter and show no distinct minimum. The gap in the Monte Carlo data is because no clusters of that size were observed in the course of the simulation. The difference between the monomer and aggregate standard chemical potential is comparable for the simulation and mean-field theory.

There are probably two reasons for the differences in the chemical potentials as a function of  $N$  for large  $N$ . The first one, which has already been discussed, is due to the non-spherical geometry of the aggregates in the simulations. Indeed, it has been shown for cylindrical aggregates that the standard chemical potentials predicted by the theory (in the case of sharp interfaces) is flatter than that of spherical aggregates<sup>27</sup>. The second reason is that since the solution was assumed to be ideal when the size distribution was inverted, the chemical potentials of the simulated aggregates are not exact results. In fact, the decrease of monomer concentration above the cmc clearly indicates non-ideal effects being important at least after

the cmc. These non-ideal effects are also observed in the recorded micelle-micelle and micelle-monomer radial distribution functions<sup>19</sup>.

Fig. 9 shows the cluster distributions from the simulations and from using the mean-field theory in the multiple equilibrium model, both for 1 vol. % total amphiphile. As expected, the cluster distribution for the mean-field result gives a peak at about 55 monomers which corresponds to the minimum in the standard chemical potentials. In comparison, the simulation shows a much broader peak at almost twice the aggregation number. Notably, where the mean-field theory predicts a peak in the cluster distribution, in the simulation these aggregates are rarely seen. As before, we locate the cmc by plotting the free monomer and aggregate concentration versus the total amphiphile concentration and observe where the two lines cross, see Fig. 5. Despite the poor agreement for the cluster distributions, the single chain mean-field theory predicts a cmc of 0.9 vol.%, in excellent agreement with the simulation result, which suggests that the theory successfully captures the free energy difference between monomers and aggregates.

It is important to understand why the theory predicts the cmc and the structure of the micelles with such accuracy, but does poorly for the size distribution. In order to understand this it is useful to look at the free energy differences underlying the formation of micelles from monomers (cmc) and the size distribution above the cmc. In the aggregation process, the free energy change is of the order of  $k_B T$  per segment. This is a very large change mostly dominated by the change in solubility of the hydrophobic segments<sup>43,44</sup>. The theory is capable of capturing that change quantitatively due to the proper counting of interactions in the bulk solvent and in the aggregate. The size distribution however arises from much smaller changes in free energy associated with small differences in the packing environment and the free energy associated with shape fluctuations, see Fig. 9. As can be seen, these changes are of the order of a fraction of  $k_B T$  per *molecule* (compare with the  $k_B T$  per *hydrophobic monomer* responsible for the cmc). Furthermore, it is clear that in the simulations there seems to be an important interaggregate interaction that qualitatively changes the size distribution of the aggregates. Note that these interactions are also probably small in magnitude as compared with the free energy changes upon aggregation. However, they need to be incorporated in a theoretical approach if a full description of the phase behavior is desired.

In the dilute limit, very close to the cmc, the interaggregate interactions are probably negligible. Therefore, part of the discrepancy in the predicted cluster distributions between theory and simulations probably stems from the assumption in the mean-field theory that the aggregates are spherical. As has been mentioned, the radii of gyration in Fig. 6 show that the larger aggregates have one principal radii that is larger than the other two. By using cylinders in the mean-field calculation we expect

to find a flatter distribution for the standard chemical potentials since the cylinder can grow by increasing in length, as has been shown in earlier work for a related system<sup>27</sup>. This would be in qualitative agreement with the flat distributions found in the simulations.

The most likely form of these aggregates is that they are spherocylinders, which are cylinders capped with hemi-spheres. It is reasonable to assume that the standard chemical potential of a spherocylinder  $\mu_N^0$  for an aggregate of size  $N$  can be expressed as a linear combination of spherical and cylindrical geometries<sup>28</sup>,

$$\mu_N^0 = \frac{1}{N} [(N - M)\mu_{cyl}^0 + M\mu_{sph}^0] \quad (20)$$

where  $\mu_{cyl}^0$ ,  $\mu_{sph}^0$  are the standard chemical potentials for amphiphiles in a sphere or cylinder respectively, and  $M/2$  is the number of amphiphiles in each hemi-sphere. Another complication over a spherical geometry is that  $M$  is not known *a priori* for a fixed number of chains in the aggregate. In principle  $\mu_N^0$  should be minimized with respect to  $M$ . This is not completely trivial since  $\mu_{cyl}^0$  and  $\mu_{sph}^0$  are functions of  $M$  and the radii of the spherical and cylindrical section have to match.

## VIII. CONCLUSIONS

In this paper we investigated the aggregation behavior of a model for diblock surfactants. In particular, we studied the behavior of  $H_4T_4$ -H systems. The model used is very simple compared to real amphiphiles. There are no differences between head group-solvent interactions versus solvent-solvent interactions, there are no counterions nor effects of counterion entropy and the tail and head groups are symmetric so that both normal and inverted micelles are identical. The model does however capture many of the features seen for non-ionic amphiphiles and should thus prove to be a useful testing ground for improving theories and for understanding these systems.

Both Monte Carlo simulation and a single chain mean field theory were used to study this model. By using Monte Carlo simulation for large systems in the canonical (NVT) ensemble we found peaks in the cluster distribution indicative of micelle formation. As overall amphiphile concentration was reduced these peaks were found to remain at approximately the same cluster number. The free monomer concentration was observed to reach a maximum close to the critical micelle concentration (cmc) of 0.9 vol.% amphiphile. This observation is inconsistent with predictions from the multiple equilibrium model for which the solution is assumed to be ideal.

The aggregation results for our  $H_4T_4$  model on a lattice of coordination number 26 can be compared to the results for  $H_{10}T_{10}$  and  $H_5T_{10}$  on a lattice of coordination number 6 from reference<sup>14</sup>. Different interaction parameter sets were used in reference<sup>14</sup> for  $H_{10}T_{10}$  and  $H_5T_{10}$ .

The CMC for  $H_{10}T_{10}$  of reference<sup>14</sup> and that in our system are comparable (of the order of 1 % vol.). The preferred aggregation number in our study was around 80 amphiphiles. This compares to a preferred aggregation number of 30 and 45, respectively, for  $H_{10}T_{10}$  and  $H_5T_{10}$  in reference<sup>14</sup>. The formation of bigger aggregates for an amphiphile of nominally shorter length can be explained by the significantly higher flexibility of our higher coordination number model.

By using a single-chain mean-field theoretical approach it is possible to evaluate the behavior of isolated aggregates of a given geometry. This includes quantities such as the density profile through a micelle and the free energy of formation. For simplicity, the aggregates were taken to be spherical. Reasonable agreement is found for the density profiles as compared to simulation for small aggregates. These small aggregates were found to have cores of almost pure tail segments with a sharp interface. For the largest aggregates the Monte Carlo results gave density profiles with diffuse tail distributions and significant penetration of solvent and head segments into the core region. The mean-field theory continues to predict a core of tail segments with a sharp interface for these large aggregates. On inspection of the radii of gyration it was found that the larger aggregates prefer cylindrical over the assumed spherical geometries which explains the discrepancy between the mean-field result and simulation. Similar agreement was found between the predictions of the Leermakers-Scheutjens-Fleer self-consistent field (SCF) theory and lattice simulations<sup>14</sup>.

The standard chemical potential difference between monomers and aggregates from the single-chain mean-field theory were found to be quantitatively similar to the simulation values for the smallest aggregates, however the result from single-chain mean-field theory has a distinct minimum in contrast to the flat distribution from simulation and diverges from the simulation result for the large aggregates. This leads to a quite different predicted aggregate size distribution with a peak at approximately half the aggregate number and a much narrower peak width than was observed in the simulations. This is partly due to assuming a spherical aggregate geometry in the theory. Interestingly, the SCF theory predicts a *larger* aggregation number than that observed in the simulations for the related model studied in<sup>14</sup>. Better agreement for the cluster distributions may be obtained if a spherocylindrical geometry is assumed in the single-chain mean-field calculations.

Despite this poor cluster distribution prediction the single-chain mean-field theory gave a cmc of 0.9 vol. % in excellent agreement with the simulation value suggesting that the theory correctly predicts the free energy difference between aggregates and monomers. This contrasts sharply with the finding of<sup>14</sup> that the SCF theory predicts a CMC three to five orders of magnitude lower than that observed from the simulations. This significant improvement is due to two factors. The most important one is the overcounting of favorable interactions in the

SCF theory due to the assumption that each monomer of the chain interacts with all its available geometrical neighbors. In other words, since the basic unit of the SCF theory is a monomer interacting with the mean-field imposed by its inter and intra-molecular neighbors, the number of possible interactions per monomer considered is larger than the number of contacts possible in the real self avoiding chain. As discussed above, this is the main driving force for aggregation, and it is probably one of the main advantages of the single-chain mean-field theory over the SCF approach in that the former properly counts the number of possible contacts. The second factor is that it has been recently shown<sup>30</sup> that the stretching free energy cost associated with transferring chains from the bulk to an interface is not properly taken into account when the chains are modeled as Gaussian in an external field, while the single-chain mean-field theory provides a very good estimate due to the consideration of the self avoiding chains as the basic units interacting with the intermolecular mean-field.

The next challenging step in improving the theory will be to introduce the shape changes seen in the simulations in the theoretical framework and to take into account interaggregate interactions that could explain the clear deviations from ideality which appear in the simulations.

## IX. ACKNOWLEDGMENTS

The authors would like to acknowledge helpful discussions with Professor Daan Frenkel, Dr. Bela Mulder, and Dr. René van Roij. Research on which this paper is based was supported at Cornell by a grant from the Department of Energy (Office of Basic Energy Sciences) and at Purdue by the National Science Foundation (grant CTS-9624268). Additional support at Cornell was provided by the Petroleum Research Fund administered by the American Chemical Society. Travel support was provided by a US-The Netherlands NSF cooperative research grant. Supercomputing time was provided by the Cornell Theory Center. IS is a Camille Dreyfus Teacher-Scholar.

## X. APPENDIX

In this appendix the details of the cluster move used in this work is described. In particular we show how to modify the acceptance probabilities in order to maintain detailed balance.

We define a bond probability  $p$  which is the probability that two neighboring sites form a cluster bond. Both sites must contain molecules that are allowed to form bonds. When chains are present, if one segment of a chain becomes bonded to a cluster, then the whole chain is included. This is equivalent to setting the bond probability along the chain backbone equal to one. The probability of creating a particular configuration of clusters  $C$

from a configuration  $\Lambda$  of molecules is,

$$P[C(\Lambda)] = \sum_{\{B\} \in \mathcal{C}} p^{n_b(B)} (1-p)^{n_{nb}(B)} \quad (21)$$

where the summation is taken over the set of different bond configurations,  $\{B\}$ , that gives the same cluster configuration  $C$ , and  $n_b$ ,  $n_{nb}$  are the numbers of possible cluster bonds that are made or not made respectively. The cluster configuration, and thus the molecule configuration, is now changed to obtain a new configuration  $C'$  and  $\Lambda'$ . In particular, we will choose a move that maintains the cluster bonds within any cluster.

If we substitute the probabilities defined in Eq. (21) into the condition of detailed balance<sup>47</sup> then we get,

$$\begin{aligned} & \exp[-\beta U(\Lambda)] p^{n_b(B)} (1-p)^{n_{nb}(B)} \\ & P_{acc}[C(\Lambda) \rightarrow C'(\Lambda')] = \\ = & \exp[-\beta U(\Lambda')] p^{n_b(B')} (1-p)^{n_{nb}(B')} \\ & P_{acc}[C'(\Lambda') \rightarrow C(\Lambda)] \end{aligned} \quad (22)$$

if we assume a Boltzmann distribution of states. Rather than using the total probabilities of making a cluster distribution, we have used the more restrictive case of forcing equality for every possible cluster bond configuration,  $B$ . Since the configurations of molecules within clusters were kept constant, the only part that changes in going between the old and new states are the contacts between the different clusters. This is true both for the number of cluster bonds as well as for the change in energy since the models considered here all have nearest-neighbor interactions. We can therefore simplify Eq. (22) to obtain the following,

$$\frac{P_{acc}[C(\Lambda) \rightarrow C'(\Lambda')]}{P_{acc}[C'(\Lambda') \rightarrow C(\Lambda)]} = \frac{(1-p)^{n_{nb}(\bar{B}')} \exp[-\beta \bar{U}(\Lambda)]}{(1-p)^{n_{nb}(\bar{B})} \exp[-\beta \bar{U}(\Lambda')]} \quad (23)$$

where  $\bar{B}$  is the configuration of bonds between different clusters and  $\bar{U}$  is the corresponding energy.

To generate these cluster configurations, we use the ‘‘cluster multiple labeling technique’’ of Hoshen and Kopelman<sup>48</sup>. This technique allows a cluster configuration to be generated using only one pass through the lattice by using multiple labels for any given cluster and keeping note of the labels which belong to each cluster. A random chain is picked and the cluster to which it belongs is moved one lattice site in a random direction. The number of non-bonded contacts between the displaced cluster and all other clusters is noted before and after the move. The move is then accepted or rejected based on the Metropolis acceptance criterion for Eq. (23),

$$P_{acc}(old \rightarrow new) = \min \left[ 1, \frac{(1-p)^{n_{nb}^{new}} \exp[-\beta U^{new}]}{(1-p)^{n_{nb}^{old}} \exp[-\beta U^{old}]} \right] \quad (24)$$

where the superscripts *old* and *new* refer to the old and new configurations and  $n_{nb}$  refers to the number of contacts between the displaced cluster and all the other clusters.

---

<sup>†</sup> Current address: Departament d'Enginyeria Química, Universitat Rovira i Virgili, Carretera de Salou, s/n 43006 Tarragona, SPAIN.

\* Author for correspondence. E-mail:azp2@cornell.edu

<sup>1</sup> Wennerström, H. and Lindmann, B., *Physics Reports*, **52**, 1 (1979).

<sup>2</sup> Jönsson, B.; Edholm, O.; Teleman, O., *J. Chem. Phys.*, **85**, 2259 (1986).

<sup>3</sup> Karaborni, S.; O'Connell, J.P., *Langmuir*, **6**, 905 (1990).

<sup>4</sup> Watanabe K.; Ferrario, M.; Klein, M.L., *J. Phys. Chem.*, **92**, 819 (1988).

<sup>5</sup> Smit, B., *Simulation of phase coexistence: from atoms to surfactants* (Ph.D. thesis, Shell Labs. 1990).

<sup>6</sup> Smit, B.; Hilbers, P.A.J.; Esselink, K.; Rupert, L.A.M.; van Os, N.M., *Nature*, **348**, 624 (1990).

<sup>7</sup> Smit, B.; Esselink, K.; Hilbers, P.A.J.; van Os, N.M.; Rupert, L.A.M.; Szeifer, I., *Langmuir*, **9**, 9 (1993).

<sup>8</sup> Karaborni, S.; Esselink, K.; Hilbers, P.A.J.; Smit, B.; Karthuser, J.; van Os, N.M., *Science*, **266**, 254 (1994).

<sup>9</sup> Larson, R.G.; Scriven, L.E.; Davis, H.T., *J. Chem. Phys.*, **83**, 2411 (1985).

<sup>10</sup> Care, C.M., *J. Phys. C. Solid State Phys.*, **20**, 689 (1987).

<sup>11</sup> Rodrigues, K.; Mattice, W.L., *J. Chem. Phys.*, **94**, 761 (1991).

<sup>12</sup> Stauffer, D.; Jan, N.; He, Y.; Pandley, R. B.; Marangoni, D. G.; Smith-Palmer, *J. Chem. Phys.*, **100**, 6934 (1994).

<sup>13</sup> Bernardes, A.T.; Henriques, V.B.; Bisch, P.M., *J. Chem. Phys.*, **101**, 645 (1994).

<sup>14</sup> Wijmans, C.; Linse, P., *Langmuir*, **11**, 3748 (1995).

<sup>15</sup> Larson, R.G., *J. Chem. Phys.*, **96**, 7904 (1992).

<sup>16</sup> Care, C.M., *J. Chem. Soc. Faraday Trans.*, **83**, 2905 (1987).

<sup>17</sup> Desplat, J.-C.; Care, C.M., *Molec. Phys.*, **87**, 441 (1996).

<sup>18</sup> Mackie, A.D.; Kaan, O.; Panagiotopoulos, A.Z. *J. Chem. Phys.* **104**, 3718 (1996).

<sup>19</sup> Mackie, A.D.; *Aggregation and Phase Behavior for Lattice Polymer and Amphiphile Models*, Doctoral Dissertation, Cornell Univ., (1996).

<sup>20</sup> Swendsen, R.H.; Wang, J.-S., *Phys. Rev. Letts.*, **58**, 86 (1987).

<sup>21</sup> Niedermayer, F., *Phys. Rev. Letts.*, **61**, 2026 (1988).

<sup>22</sup> Wu, D.; Chandler, D.; Smit, B., *J. Phys. Chem.*, **96**, 4077 (1992).

<sup>23</sup> McMullen III, W. E.; Gelbart, W. M.; Ben-Shaul, A., *J. Phys. Chem.*, **88**, 6649 (1984).

<sup>24</sup> Rudnick J.; Gaspari G., *Science* **237**, 384-389 (1987).

<sup>25</sup> Ben-Shaul, A.; Szeifer, I; Gelbart, W.M., *J. Chem. Phys.*, **83**, 3597 (1985).

<sup>26</sup> Szeifer, I.; Ben-Shaul, A.; Gelbart, W.M., *J. Chem. Phys.*, **83**, 3612 (1985).

- <sup>27</sup> Szleifer, I.; Ben-Shaul, A.; Gelbart, W.M., *J. Chem. Phys.*, **86**, 7094 (1987).
- <sup>28</sup> Szleifer, I. *Statistical thermodynamics of amphiphilic aggregates* (Ph.D. thesis, Hebrew University, 1988).
- <sup>29</sup> Carignano, M. A.; Szleifer, I., *J. Chem. Phys.*, **98**, 5006 (1993).
- <sup>30</sup> I. Szleifer and M. A. Carignano. *Adv. in Chem. Phys.*, volume XCIV, chapter 3, pages 165. I. Prigogine and S. A. Rice Eds. John Wiley and Sons, New York, 1996.
- <sup>31</sup> D. R. Fattal and A Ben-Shaul. *Biophysical Journal*, 67:983, 1994.
- <sup>32</sup> Scheutjens, J. M. H. M.; Fleer, G. J., *Macromolecules*, **83**, 1619 (1979).
- <sup>33</sup> Scheutjens, J. M. H. M.; Fleer, G. J., *J. Phys. Chem.*, **84**, 178 (1980).
- <sup>34</sup> Leermakers, F., *Statistical thermodynamics of association colloids* (Ph.D. thesis, Agricultural University, The Netherlands, 1988).
- <sup>35</sup> DiMarzio, E. A.; Rubin, R. J., *J. Chem. Phys.*, **55**, 4318 (1971).
- <sup>36</sup> Rosenbluth, M.N.; Rosenbluth, A.W., *J. Chem. Phys.*, **23**, 356 (1955).
- <sup>37</sup> In general the "ran2" random number generator from *Numerical Recipes*<sup>38</sup> was used, however we also tried "drand48" on the IBM RS6000 machines.
- <sup>38</sup> Press, W. H.; Teukolsky, S. A.; Vetterling, W. T.; Flannery, B. P., *Numerical Recipes, second edition* (Cambridge University Press, 1992).
- <sup>39</sup> Ruckenstein, E.; Nagarajan, R., *J. Phys. Chem.*, **79**, 2622 (1975).
- <sup>40</sup> Nagarajan, R.; Ruckenstein, E., *J. Colloid Interface Sci.*, **91**, 500 (1983).
- <sup>41</sup> van Os, N. M.; Daane, G. J.; Bolsman, T. A. B. M., *J. Coll. and Int. Sci.*, **123**, 267 (1988).
- <sup>42</sup> van Os, N. M.; Daane, G. J.; Haandrikman, G., *J. Coll. and Int. Sci.*, **141**, 199 (1991).
- <sup>43</sup> Tanford C. *The hydrophobic effect* Wiley, New York 1980.
- <sup>44</sup> Israelachvili J. *Intermolecular and Surface Forces* 2nd ed. Academic Press 1992.
- <sup>45</sup> Brindle, D.; Care, C.M., *J. Chem. Soc. Faraday Trans.*, **88**, 2163 (1992).
- <sup>46</sup> Wang, Y.; Mattice, W.L.; Napper, D.H., *Langmuir*, **9**, 66 (1993).
- <sup>47</sup> Allen, M.P. and Tildesley D.J., *Computer Simulation of Liquids* (Clarendon Press, Oxford, 1987).
- <sup>48</sup> Hoshen J.; Kopelman R., *Phys. Rev. B*, **14**, 3438 (1976).

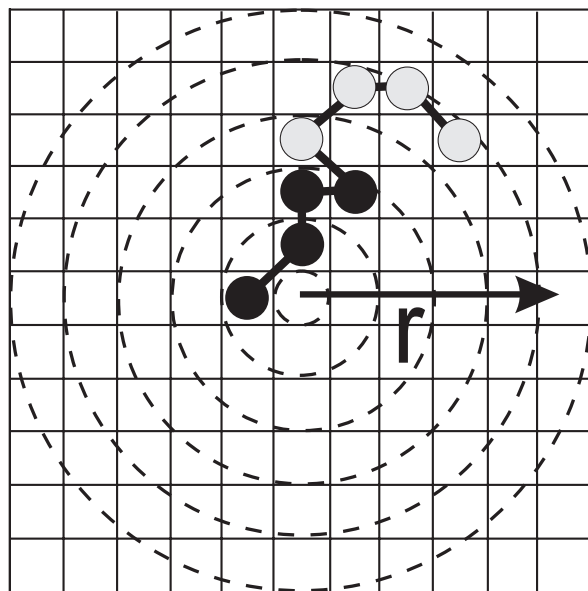


FIG. 1. Schematic diagram showing the division of a two-dimensional lattice into circular shells for the generation of density profiles.

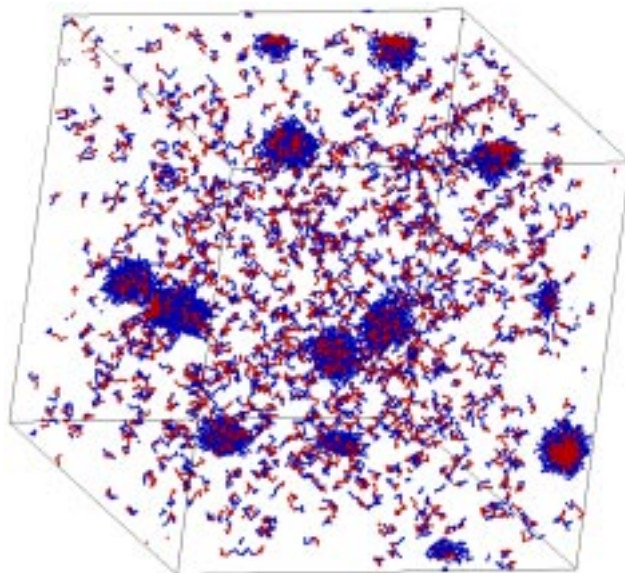


FIG. 2. Configuration of a  $120^3$  lattice with 1 vol.% amphiphile in water. Head segments are shaded dark grey, tail segments are shaded light grey and water sites are left blank.

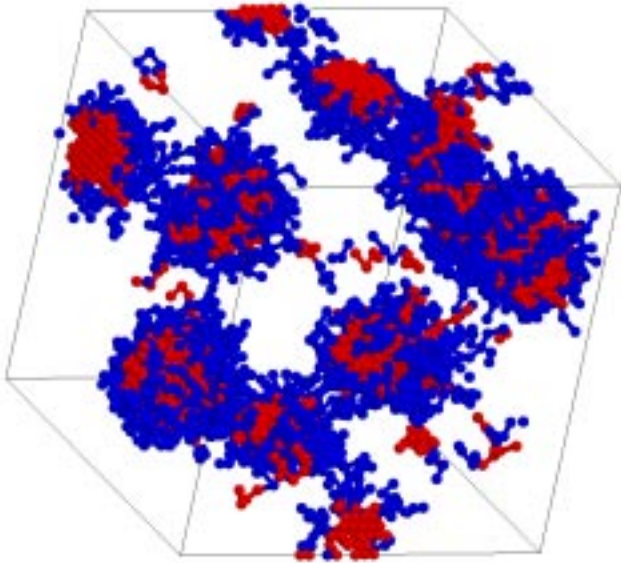


FIG. 3. Configuration of a  $40^3$  lattice with 8 vol.% amphiphile in water. Head segments are shaded dark grey, tail segments are shaded light grey and H solvent sites are left blank.

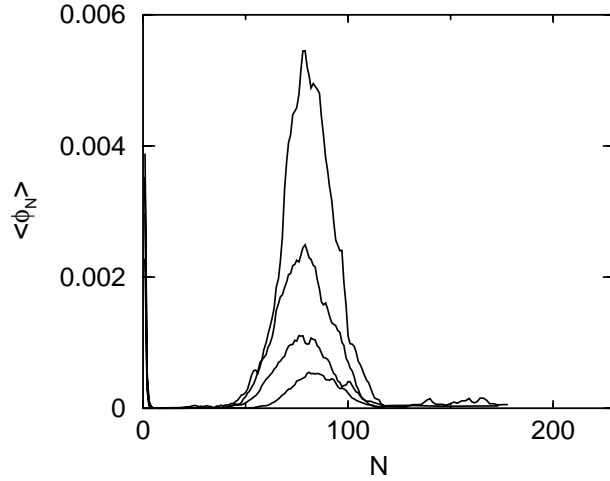


FIG. 4. Aggregate volume fraction  $\langle \phi_N \rangle$ , versus aggregate size,  $N$ . Curves from top to bottom are for overall amphiphile volume fractions of 16%, 8%, 4%, and 2% respectively. The raw simulation data were smoothed using a 3-point running average, for  $N$  greater than 20. Lattice sizes ranged from  $40^3$  (16%) to  $120^3$  (1%).

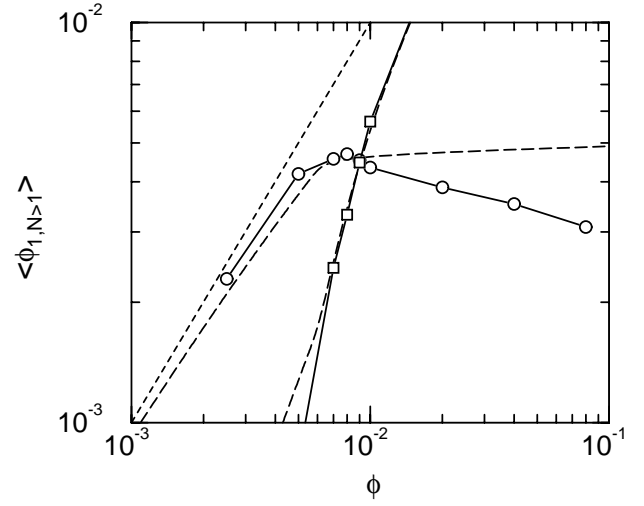


FIG. 5. Volume fraction of monomers and clusters versus the total amphiphile concentration from simulation (circles and squares, respectively) and mean-field theory augmented with the multiple equilibrium model given in Eq. (5) (long-dashed lines).

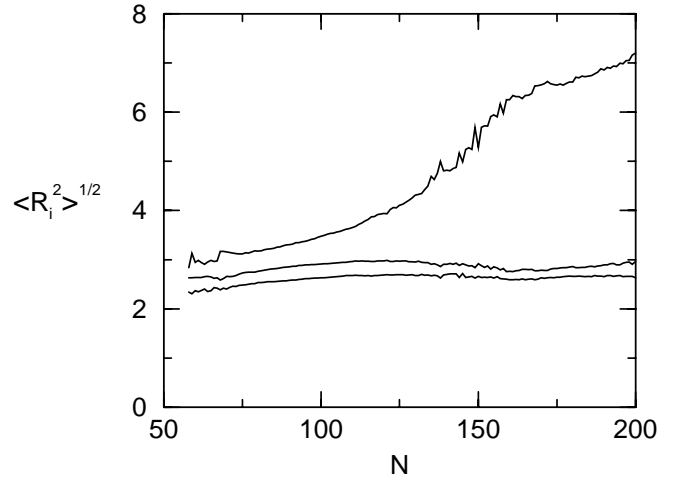


FIG. 6. Principal radii of gyration,  $\langle R_i^2 \rangle^{1/2}$ , versus aggregate size,  $N$ , for a system of 1 vol.% amphiphile.

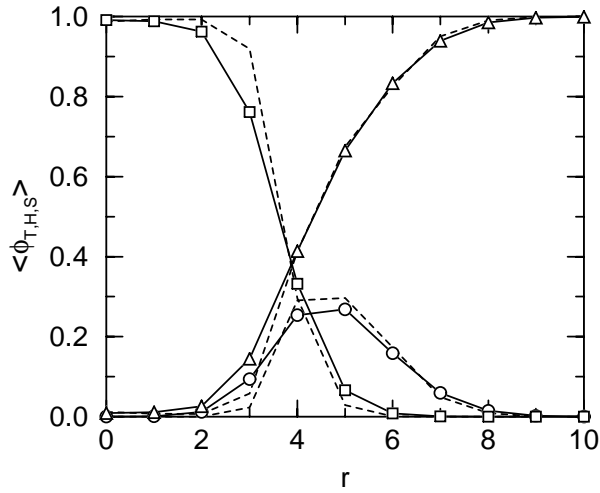


FIG. 7. Volume fraction of tail, head, and solvent,  $\langle \phi_{T,H,S} \rangle$ , versus radius,  $r$ , for the density profile through an aggregate of 80 chains: Monte Carlo results are given as solid lines with symbols and mean-field theory results by dashed lines, (square) tail sites, (circle) head sites, (triangle) solvent sites.

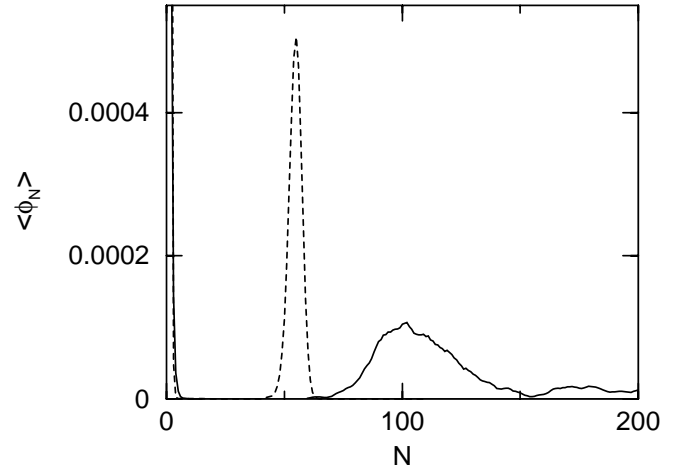


FIG. 9. Average aggregate volume fraction  $\langle \phi_N \rangle$  versus aggregate size  $N$  for 1 vol.% amphiphile in water, (—) Monte Carlo simulation, (dashed line) mean-field theory augmented with the multiple equilibrium model given in Eq. (5).

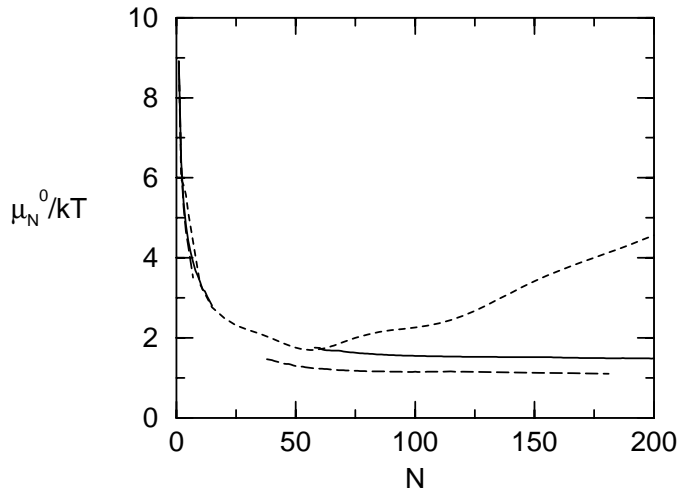


FIG. 8. Standard chemical potential,  $\mu_N^0$ , versus aggregate size,  $N$  (short-dashed line) mean-field theory (—) Monte Carlo size distribution for 1 vol.% amphiphile (long-dashed line) Monte Carlo size distribution for 8 vol.% amphiphile.